In-operando hard X-ray photoelectron spectroscopy study on the impact of current compliance and switching cycles on oxygen and carbon defects in resistive switching Ti/HfO2/TiN cells

Malgorzata Sowinska, Thomas Bertaud, Damian Walczyk, Sebastian Thiess, Pauline Calka, Lambert Alff, Christian Walczyk, and Thomas Schroeder

Articles you may be interested in

Resistive switching mechanisms relating to oxygen vacancies migration in both interfaces in Ti/HfOx/Pt memory devices
J. Appl. Phys. **113**, 064510 (2013); 10.1063/1.4791695

In-operando and non-destructive analysis of the resistive switching in the Ti/HfO2/TiN-based system by hard x-ray photoelectron spectroscopy
Appl. Phys. Lett. **101**, 143501 (2012); 10.1063/1.4756897

Hard x-ray photoelectron spectroscopy study of the electroforming in Ti/HfO2-based resistive switching structures
Appl. Phys. Lett. **100**, 233509 (2012); 10.1063/1.4728118

Semiconducting-like filament formation in TiN/HfO2/TiN resistive switching random access memories
Appl. Phys. Lett. **100**, 142102 (2012); 10.1063/1.3696672

Conducting nanofilaments formed by oxygen vacancy migration in Ti/TiO2/TiN/MgO memristive device
J. Appl. Phys. **110**, 104511 (2011); 10.1063/1.3662922

In-operando hard X-ray photoelectron spectroscopy study on the impact of current compliance and switching cycles on oxygen and carbon defects in resistive switching Ti/HfO$_2$/TiN cells

Malgorzata Sowinska,[1,a)] Thomas Bertaud,[1] Damian Walczyk,[1] Sebastian Thiess,[2] Pauline Calka,[1] Lambert Alff,[3] Christian Walczyk,[1] and Thomas Schroeder[1,4]

[1]*IHP, Im Technologiepark 25, 15236 Frankfurt (Oder), Germany*
[2]*Deutsches Elektronen-Synchrotron DESY, Notkestrasse 85, 22607 Hamburg, Germany*
[3]*Institute of Materials Science, Technische Universität Darmstadt, 64287 Darmstadt, Germany*
[4]*Brandenburgische Technische Universität, Konrad-Zuse-Strasse 1, 03046 Cottbus, Germany*

In this study, direct experimental materials science evidence of the important theoretical prediction for resistive random access memory (RRAM) technologies that a critical amount of oxygen vacancies is needed to establish stable resistive switching in metal-oxide-metal samples is presented. In detail, a novel in-operando hard X-ray photoelectron spectroscopy technique is applied to non-destructively investigates the influence of the current compliance and direct current voltage sweep cycles on the Ti/HfO$_2$ interface chemistry and physics of resistive switching Ti/HfO$_2$/TiN cells. These studies indeed confirm that current compliance is a critical parameter to control the amount of oxygen vacancies in the conducting filaments in the oxide layer during the RRAM cell operation to achieve stable switching. Furthermore, clear carbon segregation towards the Ti/HfO$_2$ interface under electrical stress is visible. Since carbon impurities impact the oxygen vacancy defect population under resistive switching, this dynamic carbon segregation to the Ti/HfO$_2$ interface is suspected to negatively influence RRAM device endurance. Therefore, these results indicate that the RRAM materials engineering needs to include all impurities in the dielectric layer in order to achieve reliable device performance. © *2014 AIP Publishing LLC*. [http://dx.doi.org/10.1063/1.4879678]

I. INTRODUCTION

The rising importance of embedded nonvolatile memory (eNVM) technologies[1] has pushed resistive random access memory (RRAM) into the spotlight. Among different oxides that show resistive switching properties, HfO$_2$ has presented a strong potential for the next generation of eNVMs due to its compatibility with Si-based complementary metal-oxide-semiconductor technology, high scalability, and low-energy dissipation.[2–4] Nonetheless, even though the resistance switching origin in bipolar HfO$_2$-based RRAMs has been investigated and mainly attributed to the rupture and regeneration at the metal/oxide interface of oxygen vacancy conductive filaments (CFs) created during the electroforming process,[5–8] the poor memory performance still delays progress in RRAM development.[9]

RRAM performance was improved thanks to the finding, which is based on the simulation of current-voltage (*I-V*) data that the size of the CFs (thus their resistance) can be controlled by tuning the voltage range[10] and/or the current compliance used during the forming/set operation.[6,11,12] Thus, in order to stabilize the resistive switching phenomenon, a critical amount of oxygen vacancies needs to be created inside the oxide film. However, this theoretical claim has not been experimentally verified yet.

We suppose that the RRAM devices performance has not been satisfactory improved yet because the previous RRAM materials science research has been mainly focused on the understanding and investigating of the exact role of oxygen vacancies, omitting the role of other HfO$_2$ film defects, which could also influence the resistive switching characteristics. Indeed, research studies not directly related to the RRAM topic report that insulating properties of HfO$_2$ can certainly be affected not only by oxygen vacancies but also other defects may change its insulating properties. For example, impurities such as carbon interstitials remained in the film after the deposition process using organic gas sources introduce impurity states in the HfO$_2$ band gap.[13–17] Furthermore, it has been shown that carbon atoms can form a permanently conducting path once they percolate.[14] Besides, although the nature of this carbon-based percolation path is not known, the high density of carbon inside HfO$_2$ might certainly promotes the breakdown because of large leakage currents.[14] We suppose that the role of other HfO$_2$ impurities on the resistive switching performance is very important and should be investigated in detail to achieve a global picture over the defect balance in HfO$_2$ films to realize reliable RRAM performance.

Therefore, in order to bring RRAM technology into a mass production, the device performance in terms of reliability has to be improved. Only by the use of a state-of-the art, novel materials science characterization technique called in-operando hard X-ray photoelectron spectroscopy (HAXPES)

---

a)Author to whom correspondence should be addressed. Electronic mail:
sowinska@ihp-microelectronics.com

at modern 3rd generation synchrotron radiation (i.e., P09 beam line at DESY in Hamburg), it is possible to directly monitor subtle changes at buried RRAM interfaces in a non-destructive way as a function of applied electrical stress to the cell with high energy resolution and sensitivity down to the impurity level. In this work, we experimentally verify the effect of current compliance and direct current (DC) voltage sweep range applied to the Ti/HfO$_2$/TiN RRAM cells during the forming/set operations on the oxygen vacancies concentration in HfO$_2$ by in-operando HAXPES[18–20] study. Additionally, the behavior of other HfO$_2$ impurities (highlighted here by carbon) at the Ti/HfO$_2$ interface is investigated as a function of current compliance and DC sweep cycling.

II. EXPERIMENTAL

The in-operando HAXPES setup used for these studies is described in Ref. 20. Three Ti/HfO$_2$/TiN samples, two $700 \times 700 \ \mu m^2$ (samples A and B) and one $700 \times 500 \ \mu m^2$ (sample C) in lateral dimensions with a $200 \times 200 \ \mu m^2$ bottom electrode contact, were investigated. All samples were prepared with amorphous HfO$_2$ films deposited by atomic vapor deposition (AVD) using tetrakis(ethylmethylamido)-hafnium Hf[N(MeEt)]$_4$ (TEMAHf) precursor; details of the HfO$_2$ deposition process (oxygen pressure, temperature, etc.) can be found in Ref. 21. X-ray photoelectron spectroscopy analysis indicates that such prepared HfO$_2$ film under back-end of line conditions contains typically about 6% of nitrogen and 4% of carbon impurities.[21]

Sample A with layer thicknesses of 10/18/67 nm was investigated at constant excitation energy of 7 keV. The HAXPES spectra were recorded for as-deposited-, OFF- and ON-states (while the current compliance (CC) was set at 0.4 mA and DC voltage was swept between −1.3 and +1.3 V). The information depth (ID), defined as three times the inelastic mean free path values (IMFP) times sinus of the electron take-off angle (TOA), was varied by three electron TOAs of 45°, 65°, and 80°. The corresponding IDs calculated for the Hf $4d_{5/2}$ core level in a Ti matrix using the TPP-2M formula from Ref. 22 are equal to 21.3, 27.6, and 30 nm.

Samples B and C with layer thicknesses of 10/14/112 nm were investigated at a constant excitation energy of 8 keV at normal emission geometry. The corresponding ID is equal to 33.9 nm, increasing the measurement sensitivity to the HfO$_2$ region. HAXPES spectra were collected for the as-deposited- and three ON-states (CC = 6, 20, and 30 mA) for sample B and, for sample C, for the as-deposited- and the 1st, 10th, 20th, and 120th OFF- and ON-states, while CC = 15 mA and DC voltage was swept between −3.5 and 3.5 V.

Photoelectrons were excited using a Si(311) double-crystal monochromator. The photon energy was calibrated with the Au $4f_{7/2}$ peak position (84 eV). A Shirley background was removed from all HAXPES spectra. Samples were electrically manipulated in the HAXPES vacuum chamber (pressure maintained below 10^{-8} mbar) in a DC sweep mode with a Keithley 4200 semiconductor characterization system. The signal was applied to the Ti top electrode, whereas the TiN bottom electrode was grounded.

III. RESULTS

A. Electrical characterization

1. Resistive switching at low electrical power

Because low-power dissipation RRAMs are of major application interest for eNVMs, sample A was operated with the smallest possible current compliance and DC voltage parameters allowing its resistance to switch. When the current compliance was increased to 0.4 mA and the voltage was swept between −1.3 and +1.3 V, the first reset and set processes appeared. The corresponding clockwise ($V_{reset} > 0$ and $V_{set} < 0$) bipolar resistive switching characteristic is shown in Fig. 1(a). It should be noted that no initial electro-forming process was necessary to establish the resistive switching behaviour in sample A. The resistance ratio read at 0.1 V between OFF- and ON-states (R_{OFF}/R_{ON}) is equal to 10. Unfortunately, this resistive switching event was unstable and no further switching cycles could be performed using these parameters.

2. Resistive switching with increasing electrical power

The next sample—sample B was investigated with increasing step-by-step applied electrical stress in order to find the onset of a stable resistive switching. The first clockwise bipolar resistive switching characteristic, presented in Fig. 1(b), appeared when current compliance was increased to 6 mA and the voltage was swept between −2.4 and +2.7 V. However, as in case of sample A, this first resistive switching was unstable and current compliance had to be further increased. For current compliance equal to 20 mA and a voltage sweep between −3.5 and 3.5 V, sudden increases of the current around 1.9, 2.1 and 2.3 V were observed (Fig. 1(c)). For the same DC voltage sweep parameters, the current compliance was further increased to 30 mA in order to reset the device to the OFF-state at a positive voltage polarity (Fig. 1(d)). After that, sample B showed stable clockwise bipolar resistive switching with a R_{OFF}/R_{ON} ratio measured at 0.1 V equal to 11.
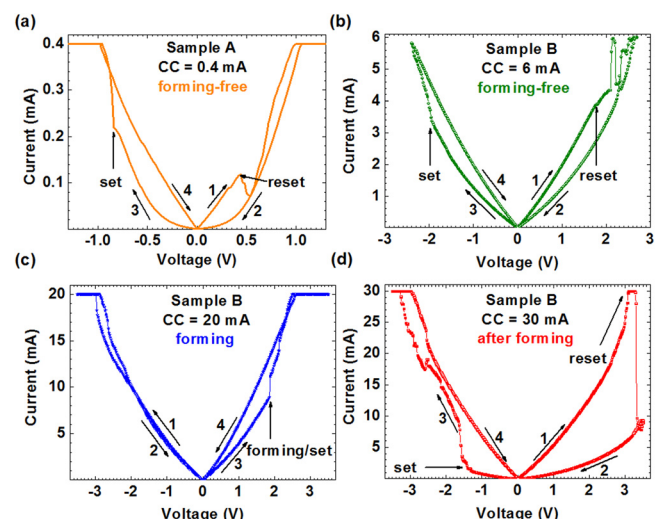
FIG. 1. *I-V* characteristics of sample A (a) and sample B (b)–(d).
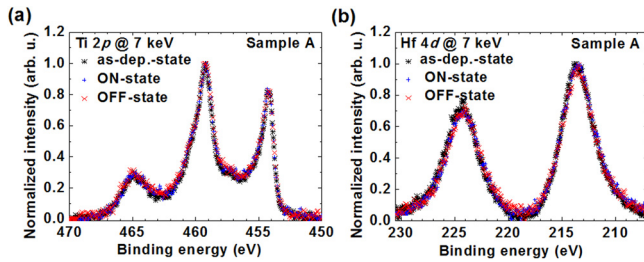
FIG. 2. Ti 2*p* (a) and Hf 4*d* (b) HAXPES spectra of sample A in the as-deposited-, ON- and OFF-states, recorded at excitation energy of 7 keV at an electron take-off angle of 80°.

B. HAXPES characterization

1. Materials changes induced by low electrical power

Figures 2(a) and 2(b) present the Ti 2*p* and Hf 4*d* emission lines recorded for the as-deposited-, OFF- and ON-states of sample A at 80° of TAO. Unlike the peak shifts in HAXPES spectra arising from Ti oxidation/reduction processes at the Ti/HfO$_2$ interface observed at higher current compliance and voltages,[19,20] sample A did not indicate any significant differences between the different resistive states. The same observation is obtained for the other two TAOs of 45° and 65° (results not shown). These results indicate that for CC = 0.4 mA, an unstable resistive switching behaviour of sample A is observed but materials changes at the Ti/HfO$_2$ interface region are below the HAXPES detection sensitivity.

2. Materials changes induced by increasing electrical power

A different situation is observed in the HAXPES spectra of sample B. Shown in Fig. 3 are the Ti 2*p* spectra of the as-deposited- and three low-resistive-states (ON-states) of sample B limited by current compliance equal to 6, 20, and 30 mA. By fitting the spectra with 5 doublet components attributed to the different Ti oxidation states (0 to +4), the metallic Ti (Ti^0) to the sum of Ti oxides (Ti^{1+}–Ti^{4+}) ratio (Ti/TiO$_y$) is calculated. The values are summarized in the inset table shown in Fig. 3. A clear monotonous decrease of the Ti/TiO$_y$ ratio from 0.60 (as-deposited-state) to 0.52 (ON-state 30 mA) is observed. This result indicates that by
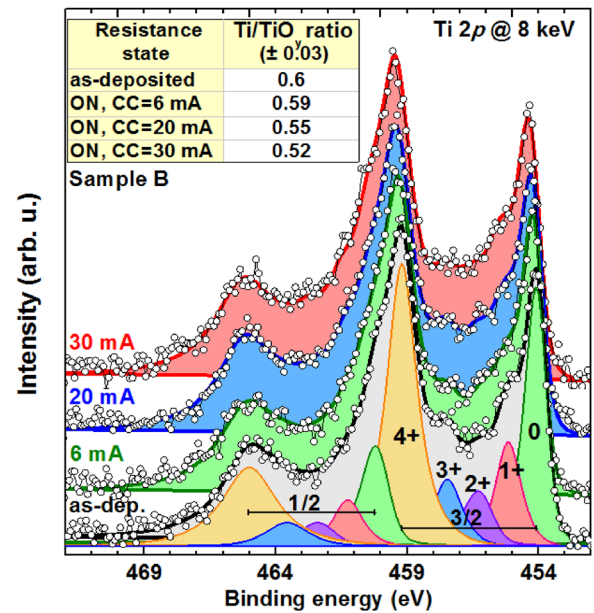
FIG. 3. Ti 2*p* HAXPES spectra of sample B in different resistive states: as-deposited-, and three ON-states (CC = 6, 20, and 30 mA) taken at 8 keV excitation energy at normal emission geometry. Spectra are fitted with five doublet components attributed to the different oxidation states of Ti (Ti^0–Ti^{4+}). Dots correspond to the experimental points and lines to fitting results. Inset presents metallic Ti (Ti^0) to total Ti oxides (Ti^{1+}–Ti^{4+}) ratio (Ti/TiO$_y$).

increasing current compliance and voltage values during the forming/set process, the Ti/HfO$_2$ interface oxidation is enhanced so that Ti gets oxidized and, in consequence, the oxygen vacancy concentration in HfO$_2$ increases. In Ref. 23, a metal-insulator transition as a function of oxygen vacancy concentration in HfO$_{2-x}$ thin films has been also observed.

An increased oxygen vacancy concentration in the HfO$_2$ film at the interface with Ti should also increase the calculated binding energy (BE) of hafnium photoemission lines in HAXPES spectra.[19,20] It was proven by measuring the BE values of the hafnium oxide in the O 1*s* and Hf 4*f* regions. All O 1*s* spectra shown in Fig. 4(a) are fitted with three Gaussian-Lorentzian line shape components attributed to the Ti oxides (O-Ti, 530.9 eV), hafnium oxides (O-Hf, 531.8 eV), and carbon oxides (O-C, 532.6 eV). Clearly, the total O 1*s* peak shifts to higher BE with increasing current
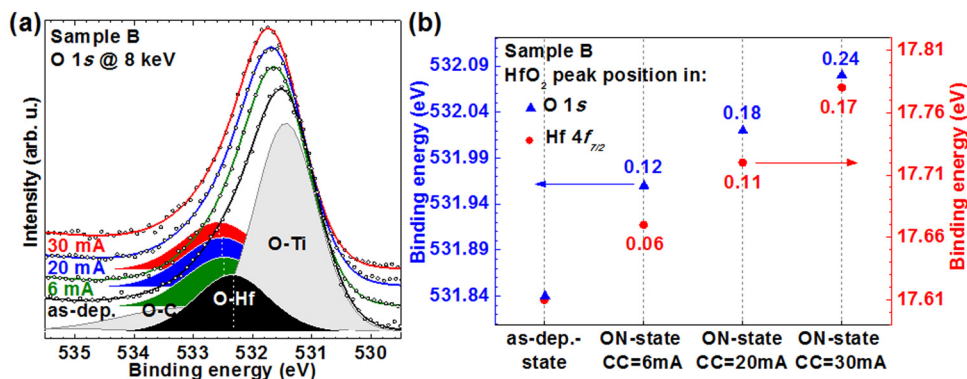
FIG. 4. (a) O 1*s* HAXPES spectra of the sample B in different resistive states: as-deposited-, and three ON-states (CC = 6, 20, and 30 mA) collected at 8 keV excitation energy at normal emission geometry. Spectra are fitted with three components attributed to the Ti oxides (O-Ti, 530.9 eV), hafnium oxides (O-Hf, 531.8 eV), and carbon oxides (O-C, 532.6 eV) features. White-dashed lines mark BE of the O-Hf component. (b) BE of hafnium oxide peaks in O 1*s* (blue triangles) and Hf 4*f$_{7/2}$* (red circles) regions. Values indicate peak shifts compared with respect to as-deposited-state peak position.

compliance. This is attributed to the BE increase of the O-Hf component, marked in Fig. 4(a) by the white-dashed line. The same monotonous BE increase presents the Hf $4f_{7/2}$ line (spectra not shown). Shown in Fig. 4(b), the BE values and the calculated peak shifts of both components move in the same direction with different amplitudes. This BE tendency allows us to conclude that the positive space charge region—related to double charged oxygen vacancies at the Ti/HfO$_2$ interface—increases with increasing electrical stress.

3. Discussion

The above results suggest that when low current compliance and voltage are used to operate an RRAM cell (sample A and first cycle of sample B), the resistive switching phenomenon is unstable. The absence of changes in the HAXPES spectra in the case of sample A indicates that only subtle modifications may have occurred in the material, however, below the detection limit of the HAXPES technique and not sufficient to stabilize the resistive switching phenomenon. By using higher current compliance and DC voltage sweep parameters during the forming/set operation of sample B, material changes at the Ti/HfO$_2$ interface are clearly detected. The observed monotonic decrease of Ti/TiO$_y$ ratio and increasing BE of hafnium oxide components in HAXPES spectra can be attributed to the increase of the positive oxygen vacancies-related space charge at the Ti/HfO$_2$ interface region (due to a Ti/HfO$_2$ redox reaction). A stable resistive switching is obtained only after a stepwise current (on positive voltage polarity) occurs in the *I-V* characteristic. We suppose that this is an electroforming process rather than a change of the switching polarity mentioned in Ref. 24, because the subsequent resistive switching is again clockwise as before. Moreover, sudden increases of the current are attributed to the growth of multiple parallel CFs between top and bottom electrodes when a sufficient amount of oxygen vacancies is created inside the oxide, supporting the hypothesis of the electroforming process.[7,25,26] Besides, first principle calculations[8] have also shown that a critical concentration of oxygen vacancies needs to be created inside the amorphous HfO$_2$ film to stabilize the resistive switching phenomenon. If the number of oxygen vacancies in the CFs is too low, the transport may be in the trap-assisted regime and dominated by the weakest link between oxygen vacancies. As the CFs thickness is increased by the addition of more oxygen vacancies, the transport gap is reduced and sizable conductivity obtained. Thus, we suppose that before the real electroforming in sample B has occurred, the number of oxygen vacancies was too small and the CFs were too weak to maintain a stable resistive switching. As the current compliance and DC sweep voltage were increased, the oxygen vacancies concentration has increased and the CFs broadened. After that, the CFs achieved an optimal morphology to support a stable resistive switching.

4. Carbon impurities

a. Carbon behavior during increasing electrical power. Besides, the in-operando HAXPES results indicate that the resistive switching does not only affect the Ti 2p, Hf

4f, and O 1s emission lines but also the C 1s. After normalization of survey scan spectra of sample B to the Hf 4d peak intensity in Fig. 5(a), it is better visible that the C 1s peak intensity increases with the increase of the electrical stress applied to the sample. Initially, for the lower current compliance and voltage sweeps, this ratio does not change significantly. However, after sample B is electroformed and shows stable resistive switching, the C 1s to Hf 4d intensity ratio (I_C/I_{Hf} in Fig. 5(a)) increases from 0.4 (as-deposited-state) to 0.6 (ON-state 30 mA). Moreover, after fitting in Fig. 5(b), the C 1s spectra with four components (assigned to the -C-C (285.5 eV), -C-O (286.5 eV), >C=O (287.5 eV), and O-COO (289.7 eV) chemical bonds[27]) show that both the concentration and the chemical environment of carbon located at the Ti/HfO$_2$ interface change. In particular, a significant increase of oxidized carbon species (here mainly >C=O) is visible by HAXPES, after sample B is set to the ON-state at CC = 30 mA.

b. Carbon behavior during DC sweep cycling. Finally, in order to further check the impact of carbon impurities during the resistive switching process, the HAXPES spectra were recorded, while cycling the RRAM cell 120 times. Shown in Fig. 6(a) are the forming-free and clockwise bipolar resistive switching characteristics of sample C as a function of the cycling number. The endurance plot, showing the current levels for ON- and OFF-states measured at 0.2 V, is presented in Fig. 6(b). As can be seen, while the ON-state current level is quasi constant, the OFF-state current level is going towards the ON-state over the cycling. In the end (120th cycle in Fig. 6(a)), the device presents a reset failure, i.e., it cannot be reset to the OFF-state. The relevant HAXPES survey scan spectra normalized to the Hf 4d peak intensity are shown in Fig. 6(c). A clear increase of the C 1s peak intensity over the cycles is observed. The calculated C 1s to Hf $4d_{5/2}$ (I_C/I_{Hf}) peaks intensity ratio (Fig. 6(c)) indicates that the cycling increases the carbon concentration at the Ti/HfO$_2$ interface. In particular, the I_C/I_{Hf} ratio increases by a factor of two from 0.51 for the as-deposited-state to 0.99 for the 120th
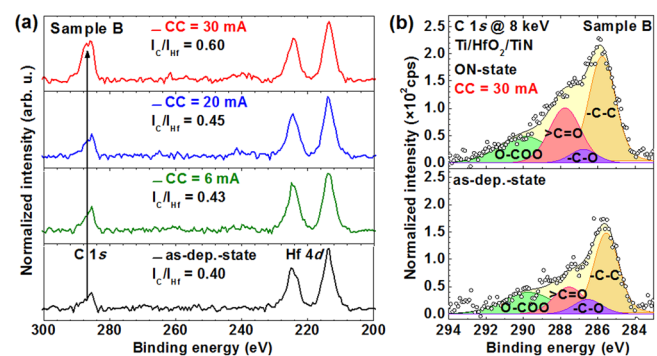
FIG. 5. (a) Survey spectra of sample B normalized to the Hf 4d peak intensity for the different resistive states: as-deposited, and three ON-states (CC = 6, 20, and 30 mA) recorded at 8 keV excitation energy at normal emission geometry. Ratios between C 1s and Hf 4d peak intensity (I_C/I_{Hf}) are indicated. (b) C 1s HAXPES spectra of sample B in the as-deposited- and ON-state (CC = 30 mA). Both spectra are fitted with four components attributed to -C-C (285.5 eV), -C-O (286.5 eV), >C=O (287.5 eV), and O-COO (289.7 eV) chemical bonds.
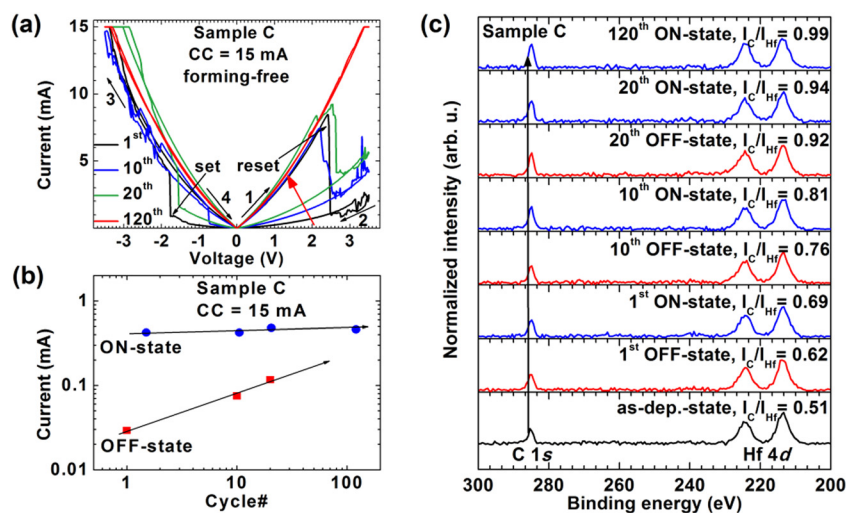
FIG. 6. (a) *I-V* characteristics showing 1st, 10th, 20th, and 120th resistive switching cycle of sample C. (b) Current levels read at 0.2 V for ON- and OFF-states. (c) Normalized survey scan spectra recorded at 8 keV of excitation energy, for as-deposited-, OFF- and ON-states of sample C (I_C/I_{Hf} ratio indicated).

ON-state. It is noted that time of flight secondary ion mass spectroscopy (ToF-SIMS) depth profiling studies (data not shown) indeed corroborate the dominant role of carbon segregation to the Ti/HfO$_2$—and not to the HfO$_2$/TiN—interface under electrical stress. These results suggest that the resistive switching may be not only based on the oxygen vacancies migration but also carbon impurities might participate to the switching mechanism, apparently in a detrimental way with respect to cell endurance, and must therefore be taken into account for memory optimization. Further impurities, i.e., like nitrogen and hydrogen might be involved in the switching physics but given ultra-low photoionization cross sections of these impurities in the high energy X-ray range, HAXPES sensitivity is limited and can thus not derive the full picture of impurity dynamics in the layer during switching.

C. Discussion

The exact role of carbon impurities in resistive switching phenomena is not clear but three different scenarios can be envisioned. First, ab-initio calculations indicate that isolated, non-reacted carbon impurities behave electronically very similar to oxygen vacancies in HfO$_2$.[28] This means that a chain of carbon impurities is capable of regular electronic transport. Especially, the creation of conductive carbon filaments, in addition to oxygen vacancies-based filaments, might be then possible and will thus certainly impact resistive switching properties. Second, Miao *et al.* reported that carbon can form defect complexes with oxygen vacancies.[14,16] In consequence, increased carbon segregation to the metal/oxide interface[15,17] can, thus, critically influence the oxygen vacancy defect population in the HfO$_2$ film. Third, another possibility of influencing the oxygen vacancies concentration in the HfO$_2$ film by carbon impurities is given by carbon oxidation in the HfO$_2$ film (see Fig. 5(b)), thus pinning the oxygen atom and suppressing, for example, its exchange with the Ti adlayer during switching. Therefore, further theoretical and experimental studies have to be done in order to understand the exact role of carbon during the resistive switching of Ti/AVD-HfO$_2$/TiN RRAM cells. Especially, how to correlate the observed increase of carbon in HAXPES

spectra with (1) an increase of sample conduction, while increasing the current compliance (Fig. 5), and (2) the OFF-state failure, while cycling the device (Fig. 6), i.e., the percolation probability of possible carbon-based filaments.

IV. SUMMARY

In summary, results of in-operando HAXPES measurements are in agreement with the theoretical predictions suggesting that the materials modifications must overcome a certain threshold (i.e., critical concentration of oxygen vacancies in the CFs) to stabilize the resistive switching phenomenon. Thus, a stable and low-power/forming-free resistive switching may be difficult to obtain when the oxygen vacancies reservoir is only based on Ti/HfO$_2$ interface redox reactions. In other words, for forming-free Ti/HfO$_2$/TiN RRAM cells, other oxygen defect engineering (e.g., trivalent cation doping) must be implemented. Finally, a further important result is that the defect physics in Ti/HfO$_2$/TiN RRAM cells is not limited to oxygen vacancies. Other impurities present in HfO$_2$ films, highlighted here by carbon, may contribute under electrical stress to the resistive switching phenomenon and, thus, influence the switching characteristics, like reliability. It is, thus, of importance to achieve a global picture of the defect physics in resistive switching HfO$_2$-based RRAM cells in order to not only understand the physics of the switching but in particular to achieve reliable RRAM performance.

[1]In *Embedded Memories for Nano-Scale VLSIs*, edited by K. Zhang (Springer, New York, 2009).

[2]Y. S. Chen, H. Y. Lee, P. S. Chen, C. H. Tsai, P. Z. Gu, T. Y. Wu, K. H. Tsai, S. S. Sheu, W. P. Lin, C. H. Lin, P. F. Chiu, W. S. Chen, F. T. Chen, C. Lien, and M.-J. Tsai, in *Proceedings of 2011 IEEE International Conference on Electron Devices Meeting (IEDM)*, 5–7 December 2011, pp. 31.3.1–31.3.4.

[3]B. Govoreanu, G. S. Kar, Z. Chen, V. Paraschiv, S. Kubicek, A. Fantini, I. P. Radu, L. Goux, S. Clima, R. Degraeve, N. Jossart, O. Richard, T. Vandeweyer, K. Seo, P. Hendrickx, G. Pourtois, H. Bender, L. Altimime, D. J. Wouters, J. A. Kittl, and M. Jurczak, in *Proceedings of 2011 IEEE International Conference on Electron Devices Meeting (IEDM)*, 5–7 December 2011, pp. 31.6.1–31.6.4.

[4]D. Walczyk, T. Bertaud, M. Sowinska, M. Lukosius, M. A. Schubert, A. Fox, D. Wolansky, A. Scheit, M. Fraschke, G. Schoof, C. Wolf, R. Kraemer, B. Tillack, R. Korolevych, V. Stikanov, C. Wenger, T. Schroeder, and C. Walczyk, in *Proceedings of 2012 International Semiconductor Conference Dresden-Grenoble (ISCDG)*, 24–26 September 2012, pp. 143–146.

[5]D. Ielmini, IEEE Trans. Electron Devices **58**, 4309 (2011).

[6]G. Bersuker, D. C. Glimer, D. Veksler, P. Kirsch, L. Vandelli, A. Padovani, L. Larcher, K. McKenna, A. Shluger, V. Iglesias, M. Porti, and M. Nafria, J. Appl. Phys. **110**, 124518 (2011).

[7]F. D. Stefano, M. Houssa, J. A. Kittl, M. Jurczak, V. V. Afanas'ev, and A. Stesmans, Appl. Phys. Lett. **100**, 142102 (2012).

[8]X. Cartoixa, R. Rurali, and J. Sune, Phys. Rev. B **86**, 165445 (2012).

[9]International technology roadmap for semiconductors (ITRS), 2012.

[10]X. Liu, K. P. Biju, J. Lee, J. Park, S. Kim, S. Park, J. Shin, S. M. Sadaf, and H. Hwang, Appl. Phys. Lett. **99**, 113518 (2011).

[11]F. Nardi, S. Larentis, S. Balatti, D. C. Gilmer, and D. Ielmini, IEEE Trans. Electron Devices **59**, 2461 (2012).

[12]S. Larentis, F. Nardi, S. Balatti, D. C. Gilmer, and D. Ielmini, IEEE Trans. Electron Devices **59**, 2468 (2012).

[13]W. S. Lau and T. Han, Appl. Phys. Lett. **86**, 152107 (2005).

[14]M. Cho, J. H. Kim, C. S. Hwang, H.-S. Ahn, S. Han, and J. Y. Won, Appl. Phys. Lett. **90**, 182907 (2007).

[15]In *Simulation of Semiconductor Processes and Devices*, edited by T. Grasser and S. Selberherr (Springer, Wien, New York, Vienna, 2007), Vol. 12, p. 165.

[16]B. Miao, R. Mahapatra, N. Wright, and A. Horsfall, J. Appl. Phys. **104**, 054510 (2008).

[17]K. Suzuki, T. Inoue, and H. Miura, in *Proceedings of International Conference on Simulation of Semiconductor Processes and Devices (SISPAD 2010)*, pp. 213–216.

[18]P. Calka, E. Martinez, D. Lafond, S. Minoret, S. Tirano, B. Detlefs, J. Roy, J. Zegenhagen, and C. Guedj, J. Appl. Phys. **109**, 124507 (2011).

[19]M. Sowinska, T. Bertaud, D. Walczyk, S. Thiess, M. A. Schubert, M. Lukosius, W. Drube, C. Walczyk, and T. Schroeder, Appl. Phys. Lett. **100**, 233509 (2012).

[20]T. Bertaud, M. Sowinska, D. Walczyk, S. Thiess, A. Gloskovskii, C. Walczyk, and T. Schroeder, Appl. Phys. Lett. **101**, 143501 (2012).

[21]C. Wenger, M. Lukosius, I. Costina, R. Sorge, J. Dabrowski, H.-J. Müssig, S. Pasko, and C. Lohe, Microelectron. Eng. **85**, 1762 (2008).

[22]S. Tanuma, C. J. Powell, and D. R. Penn, Surf. Interface Anal. **21**, 165 (1994).

[23]E. Hildebrandt, J. Kurian, M. M. Müller, T. Schroeder, H.-J. Kleebe, and L. Alff, Appl. Phys. Lett. **99**, 112902 (2011).

[24]K. Shibuya, R. Dittmann, S. Mi, and R. Waser, Adv. Mater. **22**, 411 (2010).

[25]Q. Liu, C. Dou, Y. Wang, S. Long, W. Wang, M. Liu, M. Zhang, and J. Chen, Appl. Phys. Lett. **95**, 023501 (2009).

[26]E. Miranda, J. Vac. Sci. Technol. B **29**, 01AD05 (2011).

[27]T. I. T. Okpalugo, P. Papakonstantinou, H. Murphy, J. McLaughlin, and N. M. D. Brown, Carbon **43**, 153 (2005).

[28]X. Cartoixa and J. Sune, private communication (2013).